Sequencing and bioinformatics analysis of miRNA from rat endplate chondrogenic exosomes

XUE-WU CHEN, QIU-WEI LI and HONG WANG

Department of Spinal Orthopedics, Yijishan Hospital of Wannan Medical College, Wuhu, Anhui 241000, P.R. China

Received September 21, 2022; Accepted March 16, 2023

DOI: 10.3892/etm.2023.11966

Abstract. Exosomes have a key role in various diseases, such as arthritis, heart disease and respiratory disease. Exosomes from various sources have also been indicated to improve intervertebral disc degeneration. However, the role of endplate chondrogenic exosomes in intervertebral disc degeneration has remained largely elusive. The aim of the present study was to compare exosomal microRNA (miRNA) expression patterns in endplate chondrocytes before and after degeneration, and their potential roles in the pathogenesis of intervertebral disc degeneration (IVDD). Endplate chondrocytes were extracted from rats and cultured to obtain pre- and post-degeneration chondrocytes. Exosomes were obtained from the chondrocytes by centrifugation. The two groups of exosomes were subjected to small RNA sequencing, miRNA identification, novel miRNA prediction, quantitative analysis of miRNA expression and differentially expressed (DE) miRNA screening, in addition to miRNA target gene (TG) prediction and TG functional annotation and enrichment analysis. The percentage of miRNAs isolated from the exosomes before and after degeneration was found to differ. A total of 58 DE miRNAs were analyzed, the expression levels of which were significantly different post-degeneration compared with pre-degeneration. Cell experiments were also performed, in which the exosomes were co-cultured with nucleus pulposus (NP) cells. The results indicated that the chondrocyte-derived exosomes were taken up by the NP cells and influenced the expression of aggrecan and collagen 1A and 2A, suggesting that they may inhibit IVDD via their action on NP cells. The specific miRNAs present in exosomes during IVDD may be used to develop new targets for the treatment and diagnosis of this condition. DE exosomal miRNAs derived from endplate cartilage pre- and post-degeneration may be associated with the risk of IVDD and could help to distinguish patients with IVDD. Furthermore, the expression of certain miRNAs may be associated with disease progression, which may contribute to understanding the pathophysiology of IVDD from an epigenetic perspective.

Correspondence to: Professor Hong Wang, Department of Spinal Orthopedics, Yijishan Hospital of Wannan Medical College, 2 Zheshan West Road, Jinghu, Wuhu, Anhui 241000, P.R. China
E-mail: a807497519@163.com

Key words: exosome, intervertebral disc degeneration, miRNA, epigenetic

Introduction

The main cause of chronic low back pain identified clinically is intervertebral disc degeneration (IVDD), which seriously affects physical and mental health and consumes a lot of manpower and financial resources every year. At present, the commonly used clinical drugs and surgical treatments are not able to fundamentally resolve the disease itself, and the recurrence rate is high. Therefore, it is particularly necessary to develop a more efficient and thorough strategy for its effective treatment. IVDD is a multifactorial etiological process, and the specific mechanism underlying it remains unclear. It is generally considered to be caused by ageing, lifestyle, genetic predisposition and certain non-physiological mechanical loads. These variables can induce an imbalance in the anabolic and catabolic environments of the extracellular matrix of the intervertebral disc, which causes the nucleus pulposus (NP) cells to undergo apoptosis, senescence and inflammation (1-3).

Exosomes are tiny extracellular vesicles with a double-layer lipid membrane structure and a diameter of 30-150 nm. They are secreted by mammals and are present in a variety of body fluids, including blood, cell fluid, breast milk and urine (4). Although they were originally considered to be cellular waste, they have since been shown to have a variety of purposes and to be crucial intercellular communication mediators in several pathological and physiological processes (5,6). Exosomes carry proteins, lipids, microRNAs (miRNAs) and some other RNAs, but a number of their biological effects have been suggested to be attributed to miRNAs, which are involved in various physiological and pathological processes (7-9). Several studies have confirmed that the miRNA components of exosomes can slow down IVDD by inhibiting the apoptosis of lumbar NP cells (10-12).

In the present study, exosomal miRNAs were isolated from chondrocytes before and after degeneration. Sequencing and bioinformatics analysis were then performed on the two groups of exosomal miRNAs. Quantitative analysis of the miRNAs was followed by the screening of differentially expressed (DE) miRNAs, prediction of miRNA target genes (TGs), as well as

the functional annotation and enrichment analysis of the DE miRNA TGs. In addition, known miRNAs were identified and new miRNAs were predicted.

Materials and methods

Animals and cell collection. One-week-old Sprague Dawley (SD) rats were used. Due to the protective effect of estrogen on chondrocytes (13), these rats were selected for use in the present study. They were donated by Nanjing Qinglongshan Zoo (Nanjing, China) and were maintained under standard specific pathogen-free conditions. The rats were housed in a stainless-steel cage with a 12-h light/dark cycle at 25˚C, 40-70% relative humidity and water and rat food pellets were given on time every day. For chondrocyte isolation, six 1-week-old female SD rats weighing ~20-30 g were selected. The rats were euthanized via the intraperitoneal injection of 200 mg/kg pentobarbital sodium, which induced respiratory arrest. After the rat lumbar vertebrae were immersed in 75% ethanol for 20 min at room temperature, lumbar tissues were harvested. The spine was then soaked in PBS and 2% penicillin/streptomycin for 10 min at 37˚C. The endplate cartilage was removed from the intervertebral discs, cut up in an Eppendorf (EP) tube and digested with 0.2% trypsin for 20 min at 37˚C. After digestion, DMEM/F-12 GlutaPlus, HEPES (cat. no. G4612; Servicebio) medium containing 15% fetal bovine serum (FBS; cat. no. SA220119; Procell) was added to the EP tube, and the supernatant was removed by centrifugation at 157 x g for 2 min at 4˚C. Removal of the supernatant was performed three times by centrifugation in the same manner. The obtained precipitate was digested with 0.2% collagenase for 4 h at 37˚C. Subsequently, the primary rat endplate chondrocytes were obtained by filtration using a 70-μm cell sieve, washed with PBS and inoculated in Petri dishes. Finally, DMEM/F12 with 15% FBS and 1% penicillin/streptomycin was added and the chondrocytes were cultured in an incubator at 37˚C with 5% carbon dioxide. The supernatant was extracted and stored at 80˚C until the cells reached 80-90% confluence. Cells were subcultured in two 10-cm dishes to 80-90% confluence and the supernatant was again collected and stored at 80˚C. Cell morphology was observed and photographic images were captured daily. The morphology of the cells was consistent with those of endplate chondrocytes. When the chondrocytes were cultured *in vitro*, fibrosis of chondrocytes became evident in the third generation, as the chondrocytes exhibited a long fusiform morphology, and the growth rate began to slow down. After the fourth passage, the cell morphology became more pronounced, and by the sixth passage, the cell morphology was mostly long fusiform, similar to fibroblast morphology. As the cells gradually differentiated, degeneration ensued. Based on the morphological appearance of the cells, third-generation chondrocytes were used as the pre-degeneration cells, and the fifth-generation chondrocytes were used as the post-degeneration cells. The cell supernatants were stored at -80˚C for 48-72 h and then added to DMEM/F12 medium with 15% FBS and 1% penicillin/streptomycin to maintain the culture. The Animal Research Committee of Yijishan Hospital of Wannan Medical College (Wuhu, China) approved the experimental protocol (approval no. LLSC-2022-099).

Exosome isolation and RNA extraction. Prior to and following degeneration, particles >0.45 μm in diameter were removed from the cell culture supernatant by passing it through a 0.45-μm filter. The purified supernatants were combined using an exoEasy membrane (cat. no. 76064; Qiagen GmbH) affinity centrifuge column with Buffer XBP (1:1), centrifuged at 500 x g for 1 min at 4˚C and then washed with Buffer XWP. The mixed exosomes were centrifuged at 4,000 x g for 5 min at 4˚C, and after changing the centrifuge tube, three independent elutions in 500 μl Buffer XE were performed. The elutes were stored at -80˚C.

TRIzol® (Thermo Fisher Scientific, Inc.) was used to extract RNA from the samples. To certify the samples for transcriptome sequencing, the purity, concentration and integrity of the RNA samples were verified by Implen ultramicroultraviolet spectrophotometry (NP40).

Western blot (WB) analysis. A lysis solution containing a protease inhibitor cocktail was used to extract the total protein from the exosomes. The lysis solution consisted of 1 ml RIPA lysate combined with 10 μl PMSF, both from Beyotime Institute of Biotechnology. After lysis, a bicinchoninic acid protein concentration assay kit (cat. no. PC0020; Solarbio) was used to detect the protein concentration according to the operating instructions of the kit. Subsequently, 20 μg total protein/lane was separated on a 10% SDS-PAGE gel and transferred to a polyvinylidene difluoride (PVDF) membrane (MilliporeSigma). The PVDF membrane was then cleaned once with TBST. Membranes were then immersed in the blocking solution (cat. no. P0023B; Beyotime Institute of Biotechnology) and blocked for 2 h at room temperature with gentle shaking, followed by washing with TBST once. After blocking, the membranes were incubated with 1:1,000 diluted anti-heat shock protein 70 (HSP70) (cat. no. 4876T), anti-alix (cat. no. 2171T), anti-flotillin-1 (cat. no. 18634T) and anti-annexin V (cat. no. 8555T; all from Cell Signaling Technology, Inc.) antibodies overnight at 4˚C. ECL WB Substrate (cat. no. PE0010; Beijing Solarbio Science & Technology Co., Ltd.) was applied to the PVDF membrane for exposure photography after incubation with horseradish peroxidase (HRP)-conjugated anti-rabbit IgG (cat. no. SE134) or HRP-conjugated anti-rat IgG secondary antibodies (cat. no. SE131; both from Beijing Solarbio Science & Technology Co., Ltd.) at room temperature for 1 h. Image processing was performed using ImageJ 1.8 software (National Institutes of Health) for gray value analysis.

Electron microscopy. Transmission electron microscopy was used to study the morphology of the exosomes. Briefly, the suspended exosomes were diluted with PBS and then each sample was put onto a carbon-coated copper grid. The exosomes were allowed to precipitate for 10 min and then the remaining solution was adsorbed with air-flow mesh paper.

Following immersion in 3% glutaraldehyde at room temperature for 5 min, the mesh was rinsed 10 times with deionized water. The copper grid was then exposed to 4% uranyl acetate solution at room temperature for 10 min followed by 1% methylcellulose solution at room temperature for 5 min. The samples were dried and inspected using transmission electron microscopy after 30 min.

Particle size analysis. ZetaView series nanoparticle tracking analyzer (Particle Metrix GmbH) was performed to examine the size distribution of the isolated exosomes. PBS was used to dilute the exosomes. ZetaView software version 8.05.11 (Particle Metrix GmbH) was used to examine the size and concentration of the nanoparticles. The Brownian motion of the extracted nanoparticles was also recorded.

Library preparation for small RNA (sRNA) sequencing and classification. Utilizing the HiSeq 2500 platform (Illumina Inc.), RNA sequencing (cat. no. R0024; Beyotime Institute of Biotechnology) was carried out. In brief, adapters were connected to the 3' and 5' ends of the RNAs. This was followed by reverse transcription (RT) for first-strand synthesis (size selection, 50-200 bp). The reaction solution was prepared according to the real-time PCR reaction system. Double-distilled water (DDH_2O), SYBRGreen qPCR Master Mix, Forward primer, Reverse primer and cDNA template were added to the PCR reaction tube and mixed thoroughly. For fragment screening, polyacrylamide gel electrophoresis was performed, with rubber cutting recycling of the fragments to produce sRNA libraries. The PCR products were purified using Agencourt AMPure XP technology (Beckman Coulter, Inc.) and library quality was evaluated. The raw sequences obtained by sequencing contained adaptor sequences or low-quality sequences. In order to ensure the accuracy of information analysis, quality control of the raw data is required to obtain high-quality sequences (that is, Clean): i) The adaptor was removed; ii) sequences shorter than 15 nucleotides or longer than 35 nucleotides were removed; iii) For each sample, the sequence with low quality value was removed; iv) reads with the content of unknown base N (N is the base that cannot be identified) greater than or equal to 10% were removed. A TruSeq PE Cluster Kit v4-cBot-HS (Illumina, Inc.) was used to cluster the index-coded samples on a cBot Cluster Generation System according to the manufacturer's instructions. The libraries were sequenced on the Illumina platform after cluster creation and single-end reads (15-35 bp) were produced. Small RNA sequencing of two samples was completed, and a total of 31.61 M Clean Reads were obtained.

Using Bowtie software (v1.0.0) (14), clean reads were filtered with the Silva, GtRNAdb, Rfam and Repbase databases to remove ribosomal RNA (rRNA) (15-18), transfer RNA (tRNA), small nuclear RNA (snRNA), small nucleolar RNA (snoRNA), other non-coding RNA (ncRNA) and repetitions. By comparing the remaining reads with the genome and known tRNAs from miRBase version 22 (http://www.mirbase.org/), known and new miRNAs were identified. For the prediction of the secondary structures of new miRNAs, Randfold software (http://bioinformatics.psb.ugent.be/supplementary_data/erbon/nov2003/) was used.

Sequencing data analysis. Reads from the reference genome were matched to mature sequences of known miRNAs using miRBase with a range of 2 nucleotides (nt) upstream and 5 nt downstream in order to identify known miRNAs, allowing at most one mismatch. The reads identified were considered to be known miRNAs. The majority of miRNA transcription start sites are found in introns, gene spacers and the reverse complementary regions of coding sequences. miRNA precursors have a distinctive hairpin shape, and splicing by Dicer/Dicer-like enzymes results in the production of mature bodies. The program miRDeep2 (19) was used to predict novel miRNA in the deep sequencing data based on the biological properties of miRNA. By comparing reads with genome position data, the miRDeep2 software identified potential precursor sequences. A Bayesian model was used to assess energy information for the precursor structure using RNAfold (version 2.1.7) (20) and the read distribution on the precursor sequence, considering features associated with miRNA synthesis, mature sequence characteristics, star sequences and loops, and thereby predict novel miRNA. miRDeep2 is mostly utilized for the prediction of miRNA in animals (19), but by modifying the parameters and altering the scoring scheme, it can also be used for the prediction of miRNA in plants (21). The miRNA expression levels of each sample were counted and then normalized using the transcript per million (TPM) method (22). The TPM normalization formula is as follows: TPM=(read count x 1,000,000)/mapped reads. The term read count represents the number of reads for a specific miRNA, and the term mapped reads represents the number of reads relative to all miRNAs.

It is important to choose appropriate software for differential expression analysis when attempting to identify DE miRNAs. For biological repeat experiments, DESeq2 (23) is appropriate, while for the acquisition of DE miRNA sets between two biological situations, differential expression analysis between sample groups may be used. EdgeR (24) can be utilized to identify DE miRNAs between two samples in studies without biological replication. In the present study, the relative expression levels of the two (groups) samples were compared using DESeq2 and the DE miRNAs were classified as upregulated or downregulated miRNAs.

The screening threshold for the discovery of DE miRNAs was based on the fold change (FC) in expression as follows: $|\log_2 (FC)| \geq 0.58$; $P<0.05$. The P-value conveys the probability of there being no difference between the two groups. The differential expression analysis of miRNA is an independent statistical test for the expression of a large number of miRNAs and false positives may exist. Therefore, the Benjamini-Hochberg method was used to correct the P-values used in the identification of DE miRNAs, and reduce the false discovery rate (FDR).

Table I. Primer sequences.

Primer	Sequence (5'-3')
GAPDH-F	GGAAAGCTGTGGCGTGAT
GAPDH-R	TCCACAACGGATACATTGGG
Col1A1-F	CCCACTGGGCTTATGATACC
Col1A1-R	GGCTCCTTCAATAGTCCGAG
Col2A1-F	TTCCTTGACATTGCACCTCT
Col2A1-R	ATCCTTCTCTTTTGCCCACA
Aggrecan-F	GGGCAGAAGAAAGATCGCT
Aggrecan-R	CTCCGTGTGGGTCTCATCG

Col, collagen; F, forward; R, reverse.

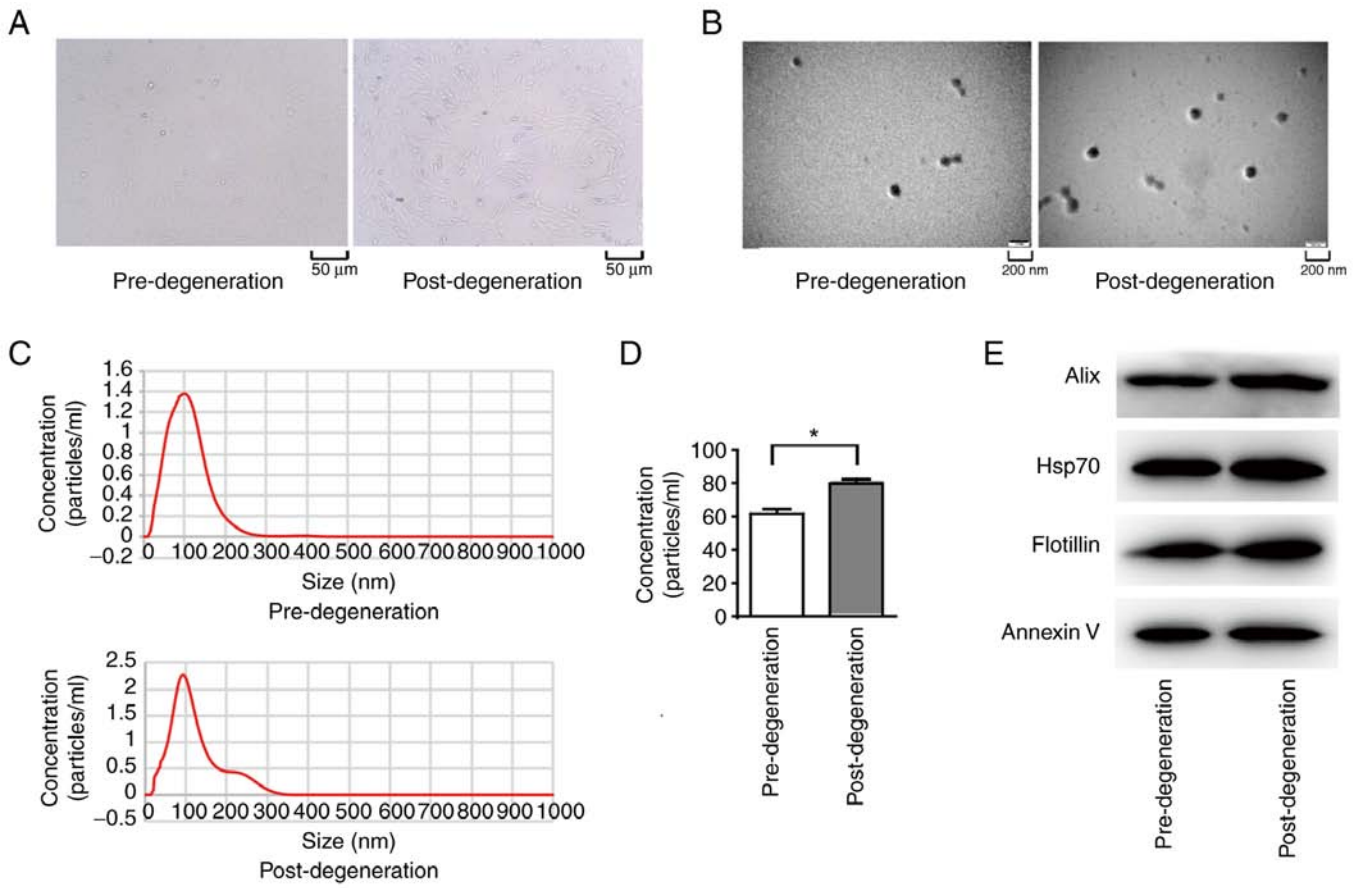

Figure 1. Identification of exosomes. (A) Light microscopy images showing the morphological differences in rat endplate chondrocytes pre- and post-degeneration (magnification, 50 μm). (B) Electron microscopy images showing exosome density before and after degeneration (magnification, 200 μm). (C) Typical results of rat chondrogenic exosome nanoparticle tracking analysis. (D) comparison of exosome concentrations before and after degeneration. (E) Exosome marker proteins identified by western blotting. *P<0.05. Hsp70, heat shock protein 70.

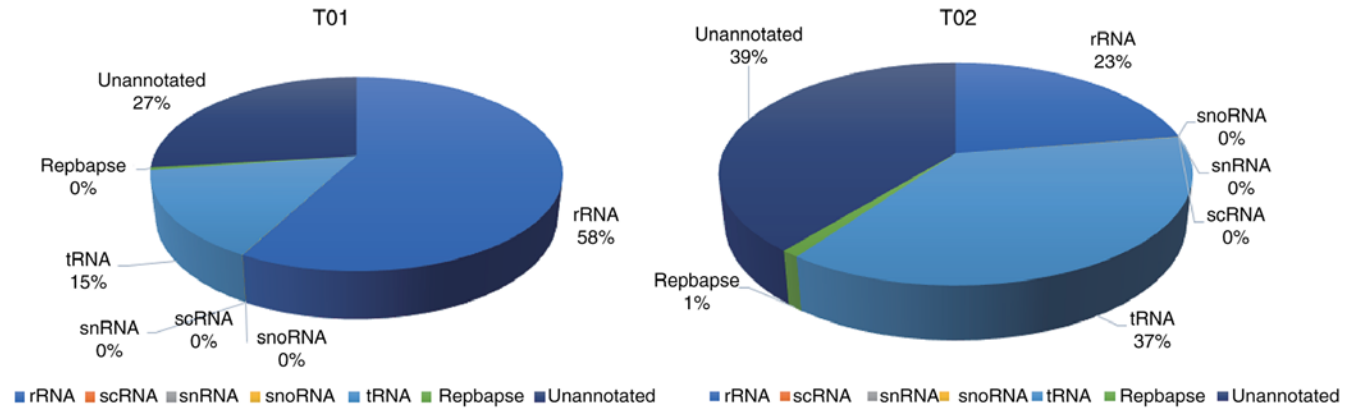

Figure 2. Small RNA classification in pre- and post-degeneration exosomes. No significant difference in the percentage of unannotated reads was detected (P=0.07). T01, before degeneration; T02, after degeneration; rRNA, ribosomal RNA; scRNA, small conditional RNA; snRNA, small nuclear RNA; snoRNA, small nucleolar RNA; tRNA, transfer RNA other non-coding RNA

miRNA TG prediction and pathway analysis. Based on gene sequencing data for the respective species and newly predicted miRNAs, miRanda (25) and TargetScan (26) were used for the prediction of TGs in animals. TG sequences were compared with the NR (27), Swiss-Prot (28), GO (29), Clusters of Orthologous Groups of Proteins (30), KEGG (31), eggNOG (32), Eukaryotic Orthologous Groups (33) and Pfam (34) databases using the BLAST program to annotate the TGs. Gene Ontology (GO) enrichment analysis (http://www.geneontology.org/) of the TGs was performed using the goseq R tool (35) to implement Wallenius non-central hypergeometric distribution-based testing. The Kyoto Encyclopedia of Genes and Genomes (KEGG) database (36) facilitates the understanding of high-level biological system functions and utilities based on molecular-level information, particularly large-scale genome sequencing datasets and other

high-throughput technologies (http://www.genome.jp/kegg/). To examine the statistical enrichment of the TGs in KEGG pathways, KOBAS (37) software was utilized.

Culture and treatment of NP cells. The caudal skin of 1-week-old SD rats was cut with a knife and the tail skin of the rats was peeled off along the incision. Two hands held the vertebral bodies on both sides of the intervertebral disc and the punctured intervertebral disc was squeezed in different directions to squeeze out the gel-like nucleus pulposus. After washing with PBS, the NP was cut into small pieces and digested with 0.5% type II collagenase (Roche Diagnostics) for 2 h at room temperature. Cells were obtained and maintained in DMEM/F12 basic medium containing 10% FBS and 100 U/ml penicillin-streptomycin in a humidified incubator containing 5% CO_2 at 37˚C.

NP cell and exosome co-culture. Exosomes were labeled with DiI (cat. no. D4010; Uelandy) for *in vivo* tracer experiments. NP cells ($1x10^6$) cultured in DMEM/F12 were seeded in a 6-well plate and then 20 μg/ml exosomes from the pre- and post-degeneration groups were added. A normal cell group comprising only NP cells was also established. The cells were harvested 48 h later and subsequently used for RT-quantitative PCR (RT-qPCR) and WB experiments.

Total RNA extraction. Nucleus pulposus cells were digested with trypsin and collected into 1.5 ml RNase-free centrifuge tubes by centrifugation at 157 x g, 5˚C for 5 min. RNA was then extracted using a Total RNA Isolation kit (cat. no. B511321; Sangon Biotech Co., Ltd.). Total RNA was extracted according to the instructions of the total RNA kit. This comprised the addition of 500 μl lysis solution to the RNA, blowing repeatedly and allowing to stand for 5-10 min at room temperature. Subsequently, 0.2 ml chloroform was added and the mixture was shaken vigorously at room temperature for 30 sec and then left at room temperature for 3 min, followed by centrifugation at 16,000 x g and 4˚C for 10 min. The upper aqueous phase was transferred to a clean centrifuge tube, and one-half volume of anhydrous ethanol was added and mixed in. This mixture was then added to the adsorption column in the collection tube using a pipette. After standing for 2 min, the tube was centrifuged at 16,000 x g for 3 min at 4˚C and the supernatant was removed. The adsorption column was again placed in the collection tube, 500 μl RPE solution was added, and after standing for 2 min and centrifugation at 11,000 x g for 30 sec at 4˚C, the supernatant was removed; this process was repeated once. The adsorption column was returned to the collection tube, centrifuged for 2 min at 11,000 x g at 4˚C and then placed in a clean 1.5-ml centrifuge tube. Finally, 30 μl diethylpyrocarbonate-treated DDH_2O was added to the center of the adsorption membrane and the RNA was centrifuged at 16,000 x g for 2 min at 4˚C. The RNA solution was stored at -70˚C for use in subsequent experiments. After total RNA was extracted, 1 μl RNA was added to a microcuvette with a German Implen ultramicroultraviolet spectrophotometer (NP40) and the absorbance was measured at wavelengths of 230, 260 and 280 nm. The machine automatically calculated and displayed the content and purity of RNA.

Table II. Top 10 most highly expressed miRNAs in pre- and post-degeneration exosomes.

Identity	T01 (TPM)	T02 (TPM)	Fold change
rno-let-7i-5p	17,707	134,531	7.60
rno-miR-21-5p	38,135	123,008	3.23
rno-miR-3473	47,884	71,730	1.50
rno-miR-148a-3p	18,536	51,394	2.77
rno-miR-26a-5p	16,315	34,505	2.11
rno-miR-99a-5p	18,769	26,776	1.43
rno-let-7b-5p	6,632	17,794	2.68
rno-miR-146a-5p	2,453	15,760	6.42
rno-miR-143-3p	11,971	8,031	0.67
rno-miR-221-3p	2,221	8,999	4.05

T01, pre-degeneration exosomes; T02, post-degeneration; TPM, transcripts per million; miRNA/miR, microRNA; rno, *Rattus norvegicus*.

Synthesis of cDNA. A cDNA synthesis kit (cat. no. AE311; TransGen Biotech) was used to synthesize cDNA from the RNA. The RT reaction mixture comprised 7 μl RNA, 1 μl random primer, 10 μl 2xES Reaction Mix, 1 μl EasyScript® RT/RI Enzyme Mix and 1 μl gDNA remover. The mixture was incubated at 25˚C for 10 min and at 42˚C for 15 min. It was then inactivated at 85˚C for 5 sec and stored at -20˚C.

qPCR amplification. The qPCR primers were synthesized by Shanghai Shenggong Biology Engineering Technology Service, Ltd. and their sequences are shown in Table I. The qPCR reaction system comprising DDH_2O, SYBR green qPCR Master Mix (cat. no. AQ101-01; TransGen Biotech), forward and reverse primers and cDNA templates was prepared, added to PCR reaction tubes and thoroughly mixed. The reaction system comprised 10 μl qPCR mix, 0.5 μl forward primer (10 μM), 0.5 μl reverse primer (10 μM), 2 μl cDNA and 7 μl nuclease-free water (total volume, 20 μl). PCR amplification was performed using the following steps: One cycle of predegeneration at 94˚C for 30 sec, and 40 cycles of denaturation at 94˚C for 5 sec and annealing at 61˚C for 35 sec. Finally, 1 cycle of melting curve analysis was performed at 97˚C for 10 sec, 65˚C for 60 sec and 97˚C for 1 sec.

Analysis of protein expression in NP cells by WB. The expression of aggrecan (cat. no. sc377219), collagen (Col)1A (cat. no. sc293182) and Col2A (cat. no. ab34712; all from Santa Cruz Biotechnology, Inc.) in NP cells cocultured with pre- and post-degeneration exosomes and the NP cell control was analyzed using the aforementioned WB procedure for exosome markers.

Fluorescence imaging. NP cells in DMEM/F12 were inoculated into the wells of a 6-well plate at a density of $5x10^5$ cells/well. The next day, green fluorescent protein (GFP) was introduced into the cells by transfection with 2 μl lentivirus phHSI-GFP (cat. no. TSPLA10289; Testobio). A fluorescence quenching agent containing DAPI was used to seal the cell layer and images were collected under a fluorescence microscope.

Table III. Differentially expressed miRNAs.

Identity	P-value	FDR	Regulated
rno-miR-1b	$6.81x10^{-86}$	$1.63x10^{-83}$	Down
rno-miR-206-3p	$3.36x10^{-47}$	$2.01x10^{-45}$	Down
rno-miR-133a-3p	$8.56x10^{-47}$	$4.10x10^{-45}$	Down
rno-miR-1-3p	$1.24x10^{-33}$	$3.29x10^{-32}$	Down
rno-let-7i-5p	$7.17x10^{-30}$	$1.72x10^{-28}$	Up
rno-miR-146a-5p	$1.72x10^{-18}$	$3.17x10^{-17}$	Up
rno-miR-29a-3p	$1.61x10^{-12}$	$2.34x10^{-11}$	Up
rno-miR-127-3p	$8.04x10^{-11}$	$1.01x10^{-9}$	Down
rno-miR-21-5p	$1.45x10^{-9}$	$1.48x10^{-8}$	Up
rno-miR-221-3p	$1.79x10^{-9}$	$1.78x10^{-8}$	Up
rno-miR-222-3p	$6.55x10^{-9}$	$6.03x10^{-8}$	Up
rno-miR-224-5p	$1.73x10^{-8}$	$1.51x10^{-7}$	Up
rno-miR-23b-3p	$1.74x10^{-7}$	$1.33x10^{-6}$	Up
rno-miR-148a-3p	$8.19x10^{-7}$	$5.85x10^{-6}$	Up
rno-miR-378a-3p	$1.05x10^{-6}$	$7.30x10^{-6}$	Down
rno-miR-125b-1-3p	$2.28x10^{-6}$	$1.56x10^{-5}$	Up
rno-miR-10a-5p	$4.12x10^{-6}$	$2.67x10^{-5}$	Down
rno-let-7c-5p	$1.05x10^{-5}$	$6.29x10^{-5}$	Up
rno-let-7b-5p	$1.17x10^{-5}$	$6.92x10^{-5}$	Up
rno-miR-143-3p	$1.36x10^{-5}$	$7.89x10^{-5}$	Down
rno-miR-199a-3p	$1.37x10^{-5}$	$7.89x10^{-5}$	Down
rno-miR-22-3p	$2.12x10^{-5}$	$1.19x10^{-4}$	Up
rno-miR-196a-5p	$2.79x10^{-5}$	$1.55x10^{-4}$	Up
rno-miR-126a-3p	$5.66x10^{-5}$	$3.01x10^{-4}$	Down
rno-miR-320-3p	$6.08x10^{-5}$	$3.20x10^{-4}$	Up
rno-miR-30a-5p	$3.02x10^{-4}$	$1.43x10^{-3}$	Up
rno-miR-133b-3p	$3.52x10^{-4}$	$1.64x10^{-3}$	Down
rno-miR-196b-5p	$4.10x10^{-4}$	$1.89x10^{-3}$	Up
rno-let-7f-5p	$4.58x10^{-4}$	$2.09x10^{-3}$	Up
rno-miR-99b-5p	$6.96x10^{-4}$	$3.00x10^{-3}$	Up
rno-miR-499-5p	$7.59x10^{-4}$	$3.21x10^{-3}$	Down
rno-miR-128-3p	$8.83x10^{-4}$	$3.68x10^{-3}$	Down
rno-miR-203a-3p	$1.65x10^{-3}$	$6.69x10^{-3}$	Down
rno-miR-26a-5p	$1.92x10^{-3}$	$7.74x10^{-3}$	Up
rno-miR-451-5p	$3.32x10^{-3}$	$1.27x10^{-2}$	Down
rno-miR-218a-5p	$3.39x10^{-3}$	$1.27x10^{-2}$	Up
rno-miR-7a-5p	$3.72x10^{-3}$	$1.38x10^{-2}$	Up
rno-miR-10b-5p	$3.88x10^{-3}$	$1.43x10^{-2}$	Up
rno-miR-184	$5.46x10^{-3}$	$1.98x10^{-2}$	Up
rno-miR-1839-5p	$5.72x10^{-3}$	$2.04x10^{-2}$	Up
rno-miR-22-5p	$6.57x10^{-3}$	$2.33x10^{-2}$	Up
rno-miR-122-5p	$6.99x10^{-3}$	$2.46x10^{-2}$	Up
rno-miR-328a-3p	$1.36x10^{-2}$	$4.66x10^{-2}$	Up
rno-miR-345-3p	$1.40x10^{-2}$	$4.67x10^{-2}$	Up
rno-miR-676	$1.40x10^{-2}$	$4.67x10^{-2}$	Down
rno-miR-16-5p	$1.41x10^{-2}$	$4.68x10^{-2}$	Up
rno-miR-149-5p	$1.53x10^{-2}$	$5.07x10^{-2}$	Up
rno-miR-145-5p	$1.62x10^{-2}$	$5.31x10^{-2}$	Down
rno-miR-139-5p	$1.73x10^{-2}$	$5.64x10^{-2}$	Down
rno-miR-182	$1.95x10^{-2}$	$6.28x10^{-2}$	Up
rno-miR-24-3p	$3.45x10^{-2}$	$1.07x10^{-1}$	Up
rno-miR-142-5p	$3.48x10^{-2}$	$1.07x10^{-1}$	Down
rno-miR-423-3p	$3.79x10^{-2}$	$1.16x10^{-1}$	Down
rno-miR-450a-5p	$4.20x10^{-2}$	$1.26x10^{-1}$	Down
rno-miR-132-3p	$4.33x10^{-2}$	$1.28x10^{-1}$	Up
rno-miR-183-5p	$4.33x10^{-2}$	$1.28x10^{-1}$	Up
rno-miR-126a-5p	$4.33x10^{-2}$	$1.28x10^{-1}$	Down
rno-miR-148b-3p	$4.43x10^{-2}$	$1.30x10^{-1}$	Up

Differentially expressed miRNAs in post-degeneration exosomes compared with pre-degeneration exosomes. miRNA/miR, microRNA; FDR, false discovery rate; rno, *Rattus norvegicus*.

Statistical analysis. The chi-square test was used to compare the percentage of unannotated reads of exosomes pre- and post-degeneration using SPSS 22.0 (IBM). Bonferroni's test was used to compare the exosome concentration, relative mRNA expression and relative protein levels between the two groups using SPSS 22.0 (IBM Corporation). Differential expression analysis of two conditions/groups was carried out using the DESeq2 R tool (version 1.10.1), which uses a model based on a negative binomial distribution to identify differential expression in digital miRNA expression data. The Benjamini-Hochberg method for reducing the FDR was used to modify the obtained P-values. DESeq2 was used to classify miRNAs with $|\log_2(FC)|\geq 0.58$; $P<0.05$ as DE miRNAs.

Results

Characterization of exosomes from endplate chondrocytes. The histological features of endplate chondrocytes before and after degeneration were examined. The number of endplate chondrocytes was lower post-degeneration than pre-degeneration, as shown in Fig. 1A. Electron microscopy showed that the exosomes obtained from the endplate chondrocytes were cup-shaped (Fig. 1B). The median diameter of the isolated exosomes was ~100 nm, according to the NTA results (Fig. 1C). The concentration of chondrogenic exosomes in the endplate increased markedly following degeneration ($P<0.01$), from ~60 mg/ml before degeneration to ~80 mg/ml after degeneration (Fig. 1D). Finally, exosome markers were examined using WB and the results revealed the presence of the exosome markers alix, HSP70, flotillin and annexin V in the particles (Fig. 1E).

sRNA classification. Numerous forms of sRNA, including miRNA, tRNA, rRNA, snRNA, snoRNA, small conditional RNA and unannotated RNAs, have been shown to be present in exosomes (38). Clean reads were filtered using various databases via the Bowtie program, which removed ncRNAs such as rRNA, tRNA, snRNA, snoRNA and repeated sequences to provide unannotated reads containing miRNA. No significant difference was detected between pre- and post-degeneration exosomes ($P=0.07$) with regard to the percentage of unannotated reads containing miRNA in the total sRNA extracted from pre- and post-degeneration exosomes, which equated to 26.89 and 39.13%, respectively (Fig. 2).

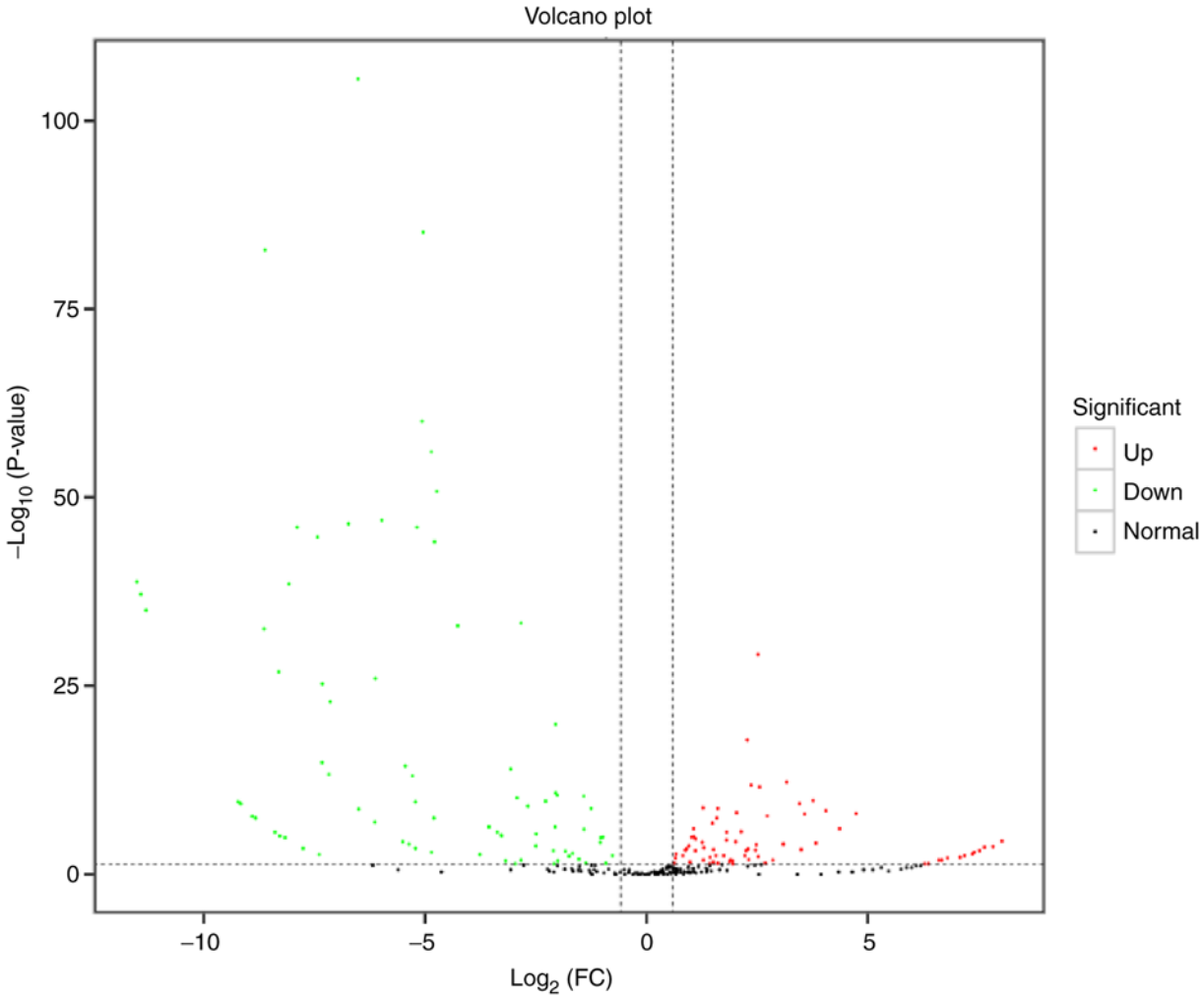

Figure 3. Volcano plot for up- and downregulated miRNAs between pre- and post-degeneration exosomes. Each point on the differential expression volcano map represents a miRNA, the horizontal coordinate is the $\log_2$(FC) in miRNA expression between the two groups and the ordinate displays the negative log of the P-value. The difference in expression between the two groups increases as the abscissa absolute value increases, and the significance of the differential expression increases with the size of the ordinate value. miRNA, microRNA; FC, fold change.

In total, sRNA sequencing was performed for the pre- and post-degeneration exosomes and a total of 479 miRNAs were found, comprising 190 newly predicted miRNAs and 289 known miRNAs 205 and 263 well-known miRNAs were detected in the exosomes pre- and post-degeneration, respectively, using miRBase 22.0 as a reference. Let-7i-5p, miR-21-5p, miR-3473, miR-148a-3p, miR-26a-5p, miR-99a-5p, let-7b-5p, miR-146a-5p, rno-miR-143-3p and rno-miR-221-3p were the top 10 miRNAs with the highest levels of expression in the pre- and post-degeneration exosomes (Table II).

DE miRNAs. The screening threshold for the discovery of DE miRNAs was $|\log_2 (FC)|\geq 0.58$; $P<0.05$. The FC of expression between the two samples and the corresponding P-value were determined for each miRNA. Post-degeneration exosomes showed 36 up- and 22 downregulated DE miRNAs compared with pre-degeneration exosomes (Table III). miR-1b, miR-206-3p, miR-133a-3p, miR-1-3p, let-7i-5p, miR-146a-5p, miR-29a-3p, miR-127-3p, miR-21-5p and miR-221-3p were the top 10 DE miRNAs. The DE miRNAs with the greatest expression FC in expression, miR-1b, has been demonstrated to inhibit apoptosis (39,40). The statistical significance of the difference between the miRNA expression levels in the two groups was determined and presented in a volcano plot (Fig. 3). An MA plot was also prepared to graphically display the general distribution of expression levels and differential multiples of DE miRNAs in the two groups (Fig. 4). Hierarchical clustering analysis was carried out on the DE miRNAs, and the miRNAs with the same or comparable expression behavior were grouped (Fig. 5).

Prediction and annotation of miRNA TGs. Based on the gene sequencing data of existing and recently identified miRNAs and associated species, TargetFinder was used to determine the TGs in plants while miRanda and Targetscan were used for TG prediction in animals. Table SI displays the anticipated TGs of each miRNA.

Annotation data were available for 14,954 of the 14,982 TGs. Table IV displays the total number of annotated TGs and the numbers of mRNAs of different lengths.

Enriched biological processes and molecular functions of genes targeted by the DE miRNAs. Enriched biological processes, molecular functions and cellular components for

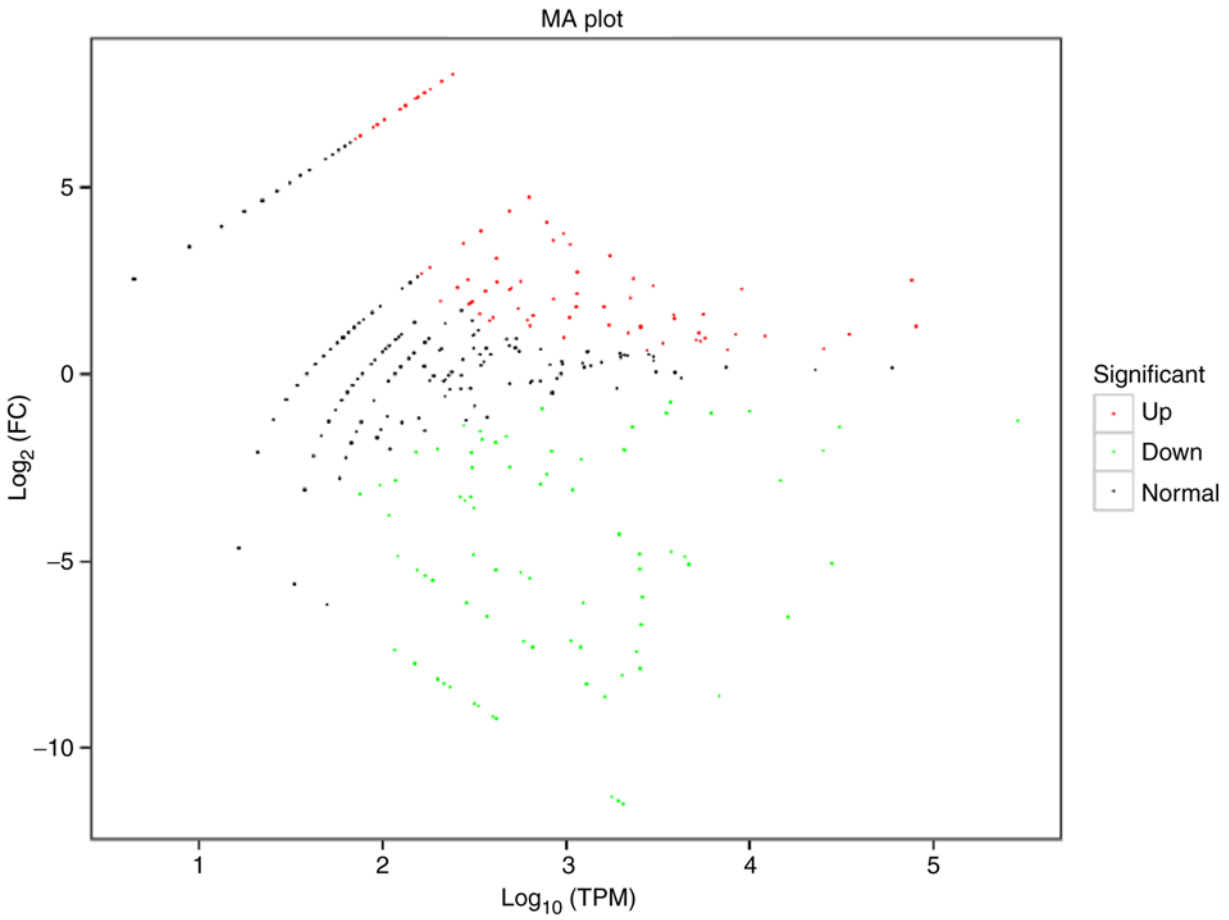

Figure 4. MA plot of differentially expressed microRNA. FC, fold change; TPM, transcripts per million.

the DE miRNAs were determined by GO analysis. The TGs of DE miRNAs in the endplate chondrocyte exosomes were found to be clearly associated with the biological processes 'biological regulation', 'signaling', 'localization', 'cellular component organization or biogenesis', 'developmental process', 'multicellular organismal process', 'response to stimulus', 'metabolic process', 'single-organism process' and 'cellular process' (Fig. 6).

'Antioxidant activity', 'structural molecule activity', 'transcription factor activity, protein binding', 'nucleic acid binding transcription factor activity', 'transporter activity', 'molecular function regulator', 'molecular transducer activity,' 'signal transducer activity', 'catalytic activity' and 'binding' are among the molecular functions found to be influenced by the predicted TGs of DE miRNAs in endplate chondrocyte exosomes (Fig. 6).

'Membrane-enclosed lumen', 'extracellular region part', 'macromolecular complex', 'membrane part', 'organelle part', 'membrane', 'organelle' and 'cell' were among the cellular components suggested to be altered by the projected TGs of DE miRNAs in the endplate chondrocyte exosomes (Fig. 6).

KEGG pathways enriched in the TGs of DE miRNAs from endplate chondrocyte exosomes. KEGG pathway analysis revealed that the TGs of the most significant miRNAs were enriched in the following pathways: 'Axon guidance', 'glutamatergic synapse', 'glycosaminoglycan biosynthesis-heparan sulfate/heparin', 'lysine degradation', 'phototransduction', 'protein digestion and absorption', 'basal cell carcinoma', 'bladder cancer', 'Hippo signaling pathway-multiple species' and 'microRNAs in cancer' (Fig. 7).

Endplate chondrocyte-derived exosomes are taken up by NP cells and influence aggrecan and Col1A and -2A expression. When chondrocyte-derived exosomes were co-cultured with NP cells, DiI-labelled pre- and post-degradation exosomes were visible by their red fluorescence in the cytoplasm of NP cells (Fig. 8A), indicating that the exosomes were taken up by the NP cells. Following the co-culture of pre- and post-degeneration exosomes with NP cells, the aggrecan and Col2A contents in the pre-degeneration exosome group were higher than those in control and post-degeneration exosome groups ($P<0.01$), while the Col1A contents in the pre-degeneration exosome group were lower than those in control and post-degeneration exosome groups ($P<0.01$; Fig. 8B and C). In addition, the RT-qPCR results indicated that the expression of aggrecan and Col2A in the pre-degeneration exosome group was higher than that in the post-degeneration exosome group ($P<0.05$), the Col1A contents in the pre-degeneration exosome group were lower than those in control groups ($P<0.01$), however, there was no significant difference in the expression of Col 1A in pre- and post-degeneration exosomes ($P>0.05$; Fig. 8D).

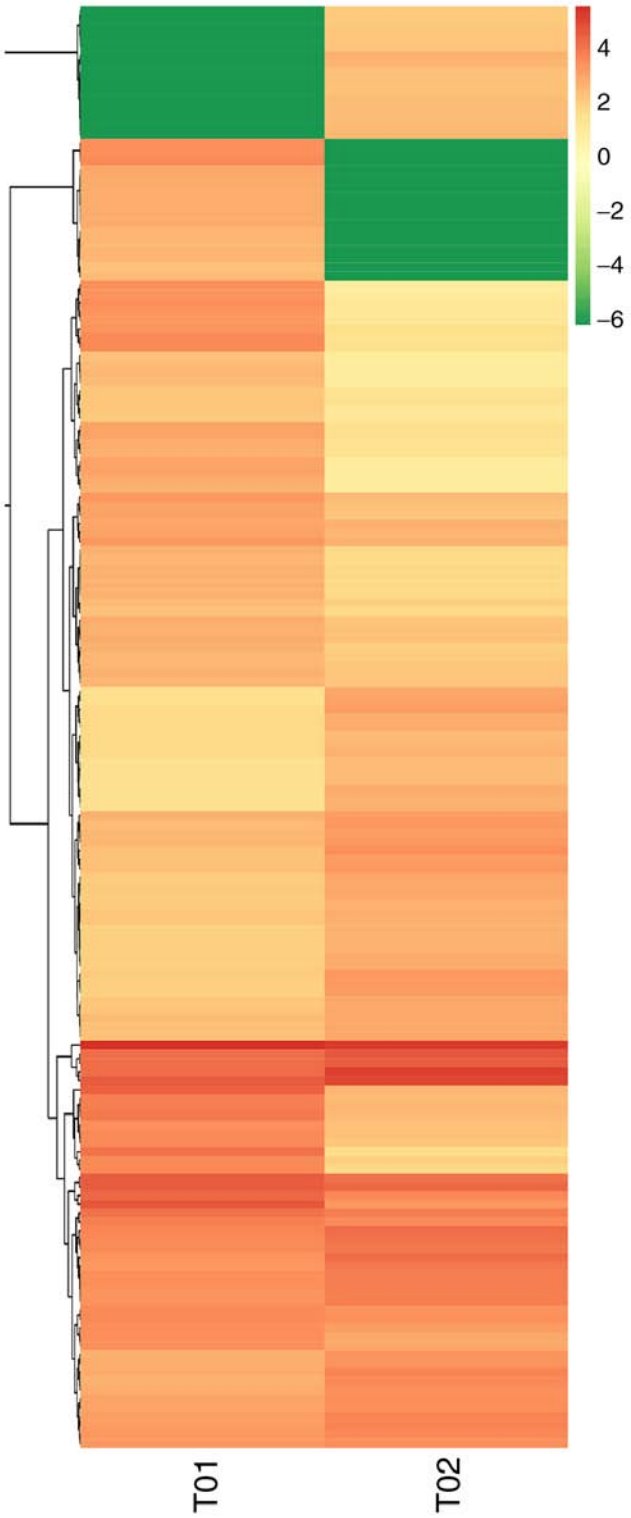

Figure 5. Differentially expressed microRNAs analyzed by hierarchical clustering. The colour represents the gene expression level in the sample-highly expressed miRNAs are displayed in red and lowly expressed miRNAs in green. T01, pre-degeneration exosomes; T02, post-degeneration exosomes.

Comparison of RNA concentration and purity after the co-culture of exosomes and NP cells. When NP cells were co-cultured with 20 μg/ml pre- and post-degeneration exosomes, the total RNA concentration in the post-degeneration exosome group was lower than that in the pre-degeneration exosome group (Table V).

Table IV. Numbers of target gene annotations and mRNAs of different lengths (n).

Annotation database	Annotated	300≤length<1,000	Length>1,000
COG	4,875	288	4,586
GO	11,534	1,250	10,266
KEGG	10,046	955	9,084
KOG	10,238	646	9,585
Pfam	14,063	1,460	12,585
Swiss-Prot	14,591	1,504	13,068
eggNOG	14,596	1,423	13,159
nr	14,934	1,633	13,270
All	14,954	1,645	13,275

COG, Clusters of Orthologous Groups of Proteins; GO, Gene Ontology; KEGG, Kyoto Encyclopedia of Genes and Genomes; KOG, Eukaryotic Orthologous Groups.

Table V. Total RNA concentration and purity.

Group	Concentration (ng/μl)	$OD_{260/280}$
Pre-degeneration exosomes	37.16	1.99
Post-degeneration exosomes	31.59	2.01
Control	59.39	2.01

$OD_{260/280}$, ratio of optical density at 260 and 280 nm.

Discussion

The results of the present study revealed that rat endplate chondrogenic exosomes have unique miRNA expression patterns before and after degeneration. sRNA sequencing was performed for the pre- and post-degeneration exosomes and a total of 479 miRNAs were found, comprising 190 newly predicted miRNAs and 289 known miRNAs. The miRNA abundance in the two types of exosomes was assessed and the DE miRNAs were identified. A total of 14,982 predicted miRNA TGs were identified, and functional annotation and enrichment analysis of the TGs were carried out. To the best of our knowledge, this is the first account of the sRNA sequencing of rat chondrogenic exosomes.

Exosomes are tiny molecular cellular vesicles that are produced by the majority of body cells and range in size from 30 to 150 nm (4-6). Proteins, lipids, metabolites, mRNAs, miRNAs and ncRNAs can be carried by exosomes (7-9). In the present study, NTA indicated that the exosomes derived from the rat endplate chondrocytes comprised 100-nm particles. In addition, the exosome markers alix, HSP70, flotillin and annexin V were detected in the particles by WB analysis, which is consistent with the recognized properties of exosomes (41).

In the present study, the chondrocyte-derived exosomal miRNA signature of the rat endplate was identified pre- and

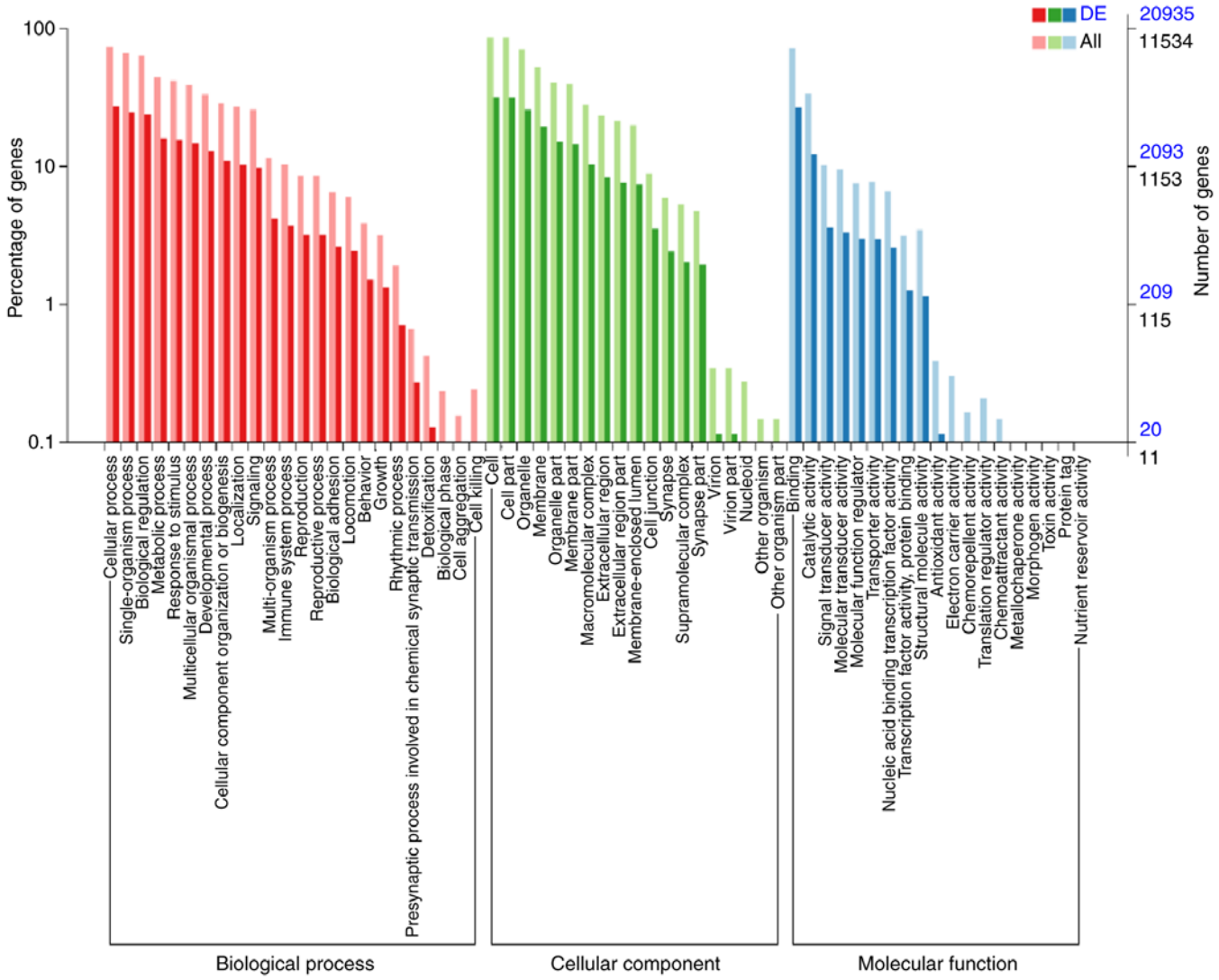

Figure 6. Gene Ontology analysis showing the major biological process, cellular component and molecular function categories predicted to be regulated by the target genes of DE microRNAs in rat endplate chondrocyte exosomes. DE, differentially expressed.

post-degeneration. The significantly upregulated miRNAs in the post-degeneration exosomes included let-7i-5p, miR-146a-5p and miR-29a-3p, and the significantly downregulated miRNAs included miR-1b, miR-206-3p, miR-133a-3p and miR-1-3p.

Among the DE miRNAs identified in the present study, miR-146a-5p and miR-222-3p have been linked to IVDD previously. According to a study conducted by Xi *et al* (42), the overexpression of HCG18 sponges miR-146a-5p in NP cells *in vitro*, thereby inhibiting proliferation by inducing S-phase cell cycle arrest and apoptosis, attracting macrophages and promoting hypercalcification. miR-146a-5p was also shown to be substantially upregulated in the knee cartilage tissues of patients with osteoarthritis in a study by Zhang *et al* (43). Furthermore, the downregulation of mir-146a-5p facilitated chondrocyte autophagy and prevented chondrocyte death *in vivo* and *in vitro*. These findings imply that chondrocyte death may be promoted by the elevated miR-146a-5p concentration of exosomes. A study by Liu *et al* (44) demonstrated that the overexpression of miR-222-3p markedly increased the apoptosis of NP cells and decreased their proliferation. The study also observed that miR-222-3p expression was much greater in degenerated intervertebral disc tissues than in normal intervertebral disc tissue, and that miR-222-3p reduced the formation of aggrecan and Col II while increasing that of matrix metalloproteinase-3. Based on these findings, we hypothesize that miR-146a-5p and miR-222-3p may be suitable IVDD therapy targets.

GO and KEGG analyses were conducted to predict the roles of the dysregulated miRNAs in IVDD. The KEGG pathways associated with the TGs of the miRNAs included 'Axon guidance', 'glutamatergic synapse', 'glycosaminoglycan biosynthesis-heparan sulfate/heparin', 'lysine degradation' and 'phototransduction'. IVDD may be associated with human brain development and mental health since axon guidance is a crucial step in the building of neuronal networks. In a bioinformatics analysis of anxiety disorder, Fan *et al* (45) found that various pathways associated neuronal brain functioning, including glutamatergic synapses and axon guidance, were significantly enriched. It is noteworthy that individuals with lower back pain

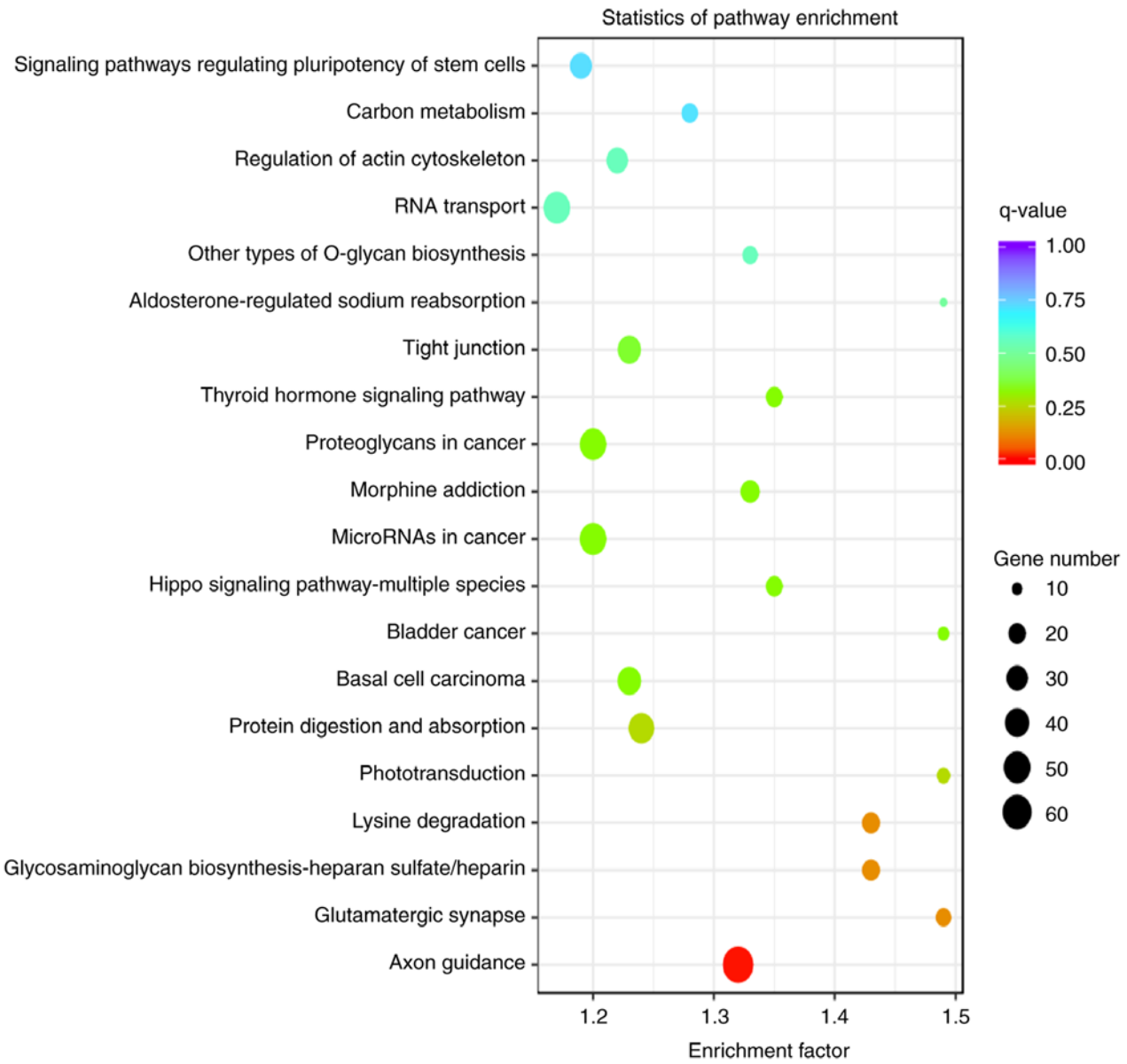

Figure 7. Kyoto Encyclopedia of Genes and Genomes Endplate pathways enriched in the target genes of differentially expressed microRNAs in rat endplate chondrocyte exosomes.

often experience anxiety and depression (46). Heparan sulfate/heparin-based glycosaminoglycan production has also been linked with IVDD. The ability of the negatively charged glycosaminoglycan side chains bound to the NP to electrostatically attach polar water molecules is crucial for maintaining adequate hydration and enabling the disc to deform reversibly under compression loads (47). The gradual loss of extracellular matrix molecules, notably glycosaminoglycan-substituted proteoglycans, is a distinguishing feature of IVDD, which often coexists with low back and neck pain (48). Exosomes may play a significant role in IVDD via the aforementioned mechanisms; however, findings concerning the effects of lysine degradation and phototransduction on IVDD are limited.

Finally, to investigate the effect of exosomes derived from endplate chondrocytes on NP cells, pre- and post-degeneration exosomes were co-cultured with NP cells, and the expression levels of aggrecan, Col1A and Col2A were analyzed using WB and RT-qPCR with GAPDH as a control. The WB results showed that the contents of aggrecan and Col2A in the pre-degeneration exosome group of NP cells were higher than those in the control and post-degeneration exosome groups, and the content of Col1A in the pre-degeneration exosome group was lower than that in the control and post-degeneration exosome groups. Assessment of the RNA extracted from the NP cells revealed that the total RNA concentrations of the pre-degeneration exosome and control groups were higher than that of the post-degeneration exosome group. In addition, RT-qPCR showed that the expression levels of aggrecan and Col2A mRNA in the pre-degeneration exosome group were higher than those in the post-degeneration exosome group, while the expression of Col1A in the pre-degeneration exosome group was lower than that in the post-degeneration exosome group. The results show that normal exosomes secreted by pre-degeneration endplate chondrocytes upregulated the protein expression levels of aggrecan and Col2A

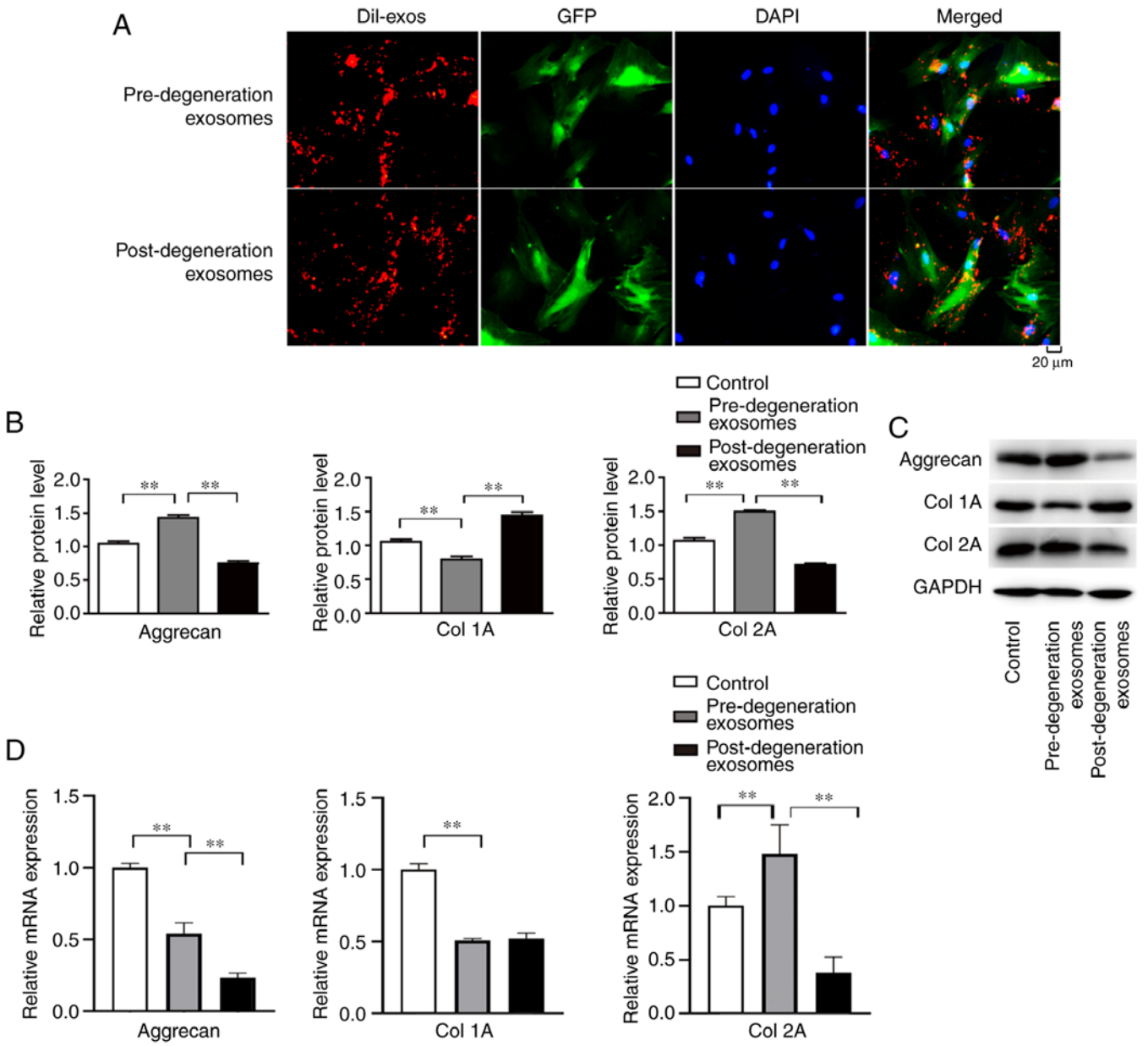

Figure 8. Exosome uptake and effects on NP cells. (A) Representative images of co-cultured NP cells and exosomes (scale bar, 20 μm). (B) Relative protein levels of aggrecan, Col1A and Col2A and (C) representative western blots for these proteins. (D) Relative mRNA expression of aggrecan, Col1A and Col2A. **P<0.01. NP, nucleus pulposus; Col, collagen; Dil-exos, exosomes labeled with cell membrane staining reagent DIL; GFP, green fluorescent protein.

and the mRNA expression of Col2A, and downregulated the protein and mRNA expression levels of Col1A in NP cells. However, following the co-culture of degraded exosomes with NP cells, the protein and mRNA expression levels of aggrecan and Col2A were decreased while those of Col1A were increased compared with the respective levels in NP cells co-cultured with pre-degeneration exosomes. These results suggest that chondrocyte-derived exosomes may enhance the proliferation of NP cells, thus playing a role in the prevention and treatment of IVDD.

It is important to consider the limitations of the present study. Although rats are among the most frequently utilized animal models of IVDD, DE miRNAs require further assessment in human exosomes as well as other animal models.

In conclusion, the present study indicates that specific miRNAs may be carried by exosomes during IVDD, which differ from those pre-degeneration. The DE miRNAs and their TGs may serve as prospective targets for the identification, prevention and treatment of IVDD. However, the functions of DE endplate chondrogenic exosomal miRNAs in the etiology of IVDD require further investigation.

Acknowledgements

The authors would like to thank Yijishan Central Laboratory of Wannan Medical College (Wuhu, China) for providing experimental equipment.

Funding

No funding was received.

Availability of data and materials

The datasets generated and/or analyzed during the current study are available in the INSDC member repository (Bank It2645413:OP866295-OP866723; https://www.ncbi.nlm.nih.gov/WebSub/) and in Table SII.

Authors' contributions

QWL was responsible for conceptualization and methodology. HW performed data curation. QWL and XWC contributed to the formal analysis. XWC acquired funding and resources and was responsible for project administration. QWL wrote the original draft of the manuscript and HW reviewed and edited the manuscript. XWC and HW confirm the authenticity of all the raw data. All authors have read and approved the final manuscript.

Ethics approval and consent to participate

The Animal Care and Use Committee and Animal Ethics Committee of Yijishan Hospital of Wannan Medical College (Wuhu, China) authorized the present study (approval no. LLSC-2022-099).

Patient consent for publication

Not applicable.

Competing interests

The authors declare that they have no competing interests.

References

1. Cazzanelli P and Wuertz-Kozak K: MicroRNAs in intervertebral disc degeneration, apoptosis, inflammation, and mechanobiology. Int J Mol Sci 21: 3601, 2020.
2. Kos N, Gradisnik L and Velnar T: A Brief review of the degenerative intervertebral disc disease. Med Arch 73: 421-424, 2019.
3. Dowdell J, Erwin M, Choma T, Vaccaro A, Iatridis J and Cho SK: Intervertebral disk degeneration and repair. Neurosurgery 80 (3S): S46-S54, 2017.
4. Yang D, Zhang W, Zhang H, Zhang F, Chen L, Ma L, Larcher LM, Chen S, Liu N, Zhao Q, *et al*: Progress, opportunity, and perspective on exosome isolation-efforts for efficient exosome-based theranostics. Theranostics 10: 3684-3707, 2020.
5. Hu Y, Zhang R and Chen G: Exosome and secretion: Action on? Adv Exp Med Biol 1248: 455-483, 2020.
6. Whitford W and Guterstam P: Exosome manufacturing status. Future Med Chem 11: 1225-1236, 2019.
7. Mori MA, Ludwig RG, Garcia-Martin R, Brandão BB and Kahn CR: Extracellular miRNAs: From biomarkers to mediators of physiology and disease. Cell Metab 30: 656-673, 2019.
8. He X, Kuang G, Wu Y and Ou C: Emerging roles of exosomal miRNAs in diabetes mellitus. Clin Transl Med 11: e468, 2021.
9. Emanueli C, Shearn AI, Angelini GD and Sahoo S: Exosomes and exosomal miRNAs in cardiovascular protection and repair. Vascul Pharmacol 71: 24-30, 2015.
10. Cheng X, Zhang G, Zhang L, Hu Y, Zhang K, Sun X, Zhao C, Li H, Li YM and Zhao J: Mesenchymal stem cells deliver exogenous miR-21 via exosomes to inhibit nucleus pulposus cell apoptosis and reduce intervertebral disc degeneration. J Cell Mol Med 22: 261-276, 2018.
11. Xu J, Xie G, Yang W, Wang W, Zuo Z and Wang W: Platelet-rich plasma attenuates intervertebral disc degeneration via delivering miR-141-3p-containing exosomes. Cell Cycle 20: 1487-1499, 2021.
12. Zhu L, Shi Y, Liu L, Wang H, Shen P and Yang H: Mesenchymal stem cells-derived exosomes ameliorate nucleus pulposus cells apoptosis via delivering miR-142-3p: Therapeutic potential for intervertebral disc degenerative diseases. Cell Cycle 19: 1727-1739, 2020.
13. Zai Z, Xu Y, Qian X, Li Z, Ou Z, Zhang T, Wang L, Ling Y, Peng X, Zhang Y and Chen F: Estrogen antagonizes ASIC1a-induced chondrocyte mitochondrial stress in rheumatoid arthritis. J Transl Med 20: 561, 2022.
14. Langmead B, Trapnell C, Pop M and Salzberg SL: Ultrafast and memory-efficient alignment of short DNA sequences to the human genome. Genome Biol 10: R25, 2009.
15. Quast C, Pruesse E, Yilmaz P, Gerken J, Schweer T, Yarza P, Peplies J and Glöckner FO: The SILVA ribosomal RNA gene database project: Improved data processing and web-based tools. Nucleic Acids Res 41 (Database Issue): D590-D596, 2013.
16. Chan PP and Lowe TM: GtRNAdb 2.0: An expanded database of transfer RNA genes identified in complete and draft genomes. Nucleic Acids Res 44 (D1): D184-D189, 2016.
17. Kalvari I, Nawrocki EP, Argasinska J, Quinones-Olvera N, Finn RD, Bateman A and Petrov AI: Non-coding RNA analysis using the Rfam database. Curr Protoc Bioinformatics 62: e51, 2018.
18. Jurka J, Kapitonov VV, Pavlicek A, Klonowski P, Kohany O and Walichiewicz J: Repbase update, a database of eukaryotic repetitive elements. Cytogenet Genome Res 110: 462-467, 2005.
19. Friedländer MR, Mackowiak SD, Li N, Chen W and Rajewsky N: miRDeep2 accurately identifies known and hundreds of novel microRNA genes in seven animal clades. Nucleic Acids Res 40: 37-52, 2012.
20. Denman RB: Using RNAFOLD to predict the activity of small catalytic RNAs. Biotechniques 15: 1090-1095, 1993.
21. Zhang Z, Jiang L, Wang J, Gu P and Chen M: MTide: An integrated tool for the identification of miRNA-target interaction in plants. Bioinformatics 31: 290-291, 2015.
22. Li B, Ruotti V, Stewart RM, Thomson JA and Dewey CN: RNA-Seq gene expression estimation with read mapping uncertainty. Bioinformatics 26: 493-500, 2010.
23. Love MI, Huber W and Anders S: Moderated estimation of fold change and dispersion for RNA-seq data with DESeq2. Genome Biol 15: 550, 2014.
24. Robinson MD, McCarthy DJ and Smyth GK: edgeR: A bioconductor package for differential expression analysis of digital gene expression data. Bioinformatics 26: 139-140, 2010.
25. Betel D, Wilson M, Gabow A, Marks DS and Sander C: The microRNA.org resource: Targets and expression. Nucleic Acids Res 36 (Database Issue): D149-D153, 2008.
26. Lewis BP, Shih IH, Jones-Rhoades MW, Bartel DP and Burge CB: Prediction of mammalian microRNA targets. Cell 115: 787-798, 2003.
27. Deng Y, Li J, Wu S, Zhu Y, Chen Y, He F, Chen Y, Deng LY, Li J and Wu S: Integrated nr database in protein annotation system and its localization. Comp Eng 32: 71-74, 2006.
28. Apweiler R, Bairoch A, Wu CH, Barker WC, Boeckmann B, Ferro S, Gasteiger E, Huang H, Lopez R, Magrane M, *et al*: UniProt: The universal protein knowledgebase. Nucleic Acids Res 32 (Database Issue): D115-D119, 2004.
29. Ashburner M, Ball CA, Blake JA, Botstein D, Butler H, Cherry JM, Davis AP, Dolinski K, Dwight SS, Eppig JT, *et al*: Gene ontology: Tool for the unification of biology. The gene ontology consortium. Nat Genet 25: 25-29, 2000.
30. Tatusov RL, Galperin MY, Natale DA and Koonin EV: The COG database: A tool for genome-scale analysis of protein functions and evolution. Nucleic Acids Res 28: 33-36, 2000.
31. Kanehisa M, Goto S, Kawashima S, Okuno Y and Hattori M: The KEGG resource for deciphering the genome. Nucleic Acids Res 32 (Database Issue): D277-D280, 2004.
32. Huerta-Cepas J, Szklarczyk D, Heller D, Hernández-Plaza A, Forslund SK, Cook H, Mende DR, Letunic I, Rattei T, Jensen LJ, *et al*: eggNOG 5.0: A hierarchical, functionally and phylogenetically annotated orthology resource based on 5090 organisms and 2502 viruses. Nucleic Acids Res 47 (D1): D309-D314, 2019.
33. Koonin EV, Fedorova ND, Jackson JD, Jacobs AR, Krylov DM, Makarova KS, Mazumder R, Mekhedov SL, Nikolskaya AN, Rao BS, *et al*: A comprehensive evolutionary classification of proteins encoded in complete eukaryotic genomes. Genome Biol 5: R7, 2004.
34. Eddy SR: Profile hidden Markov models. Bioinformatics 14: 755-763, 1998.

35. Li Y, Wang M, Li Q, Gao Y, Li Q, Li J and Cao Y: Transcriptome profiling of longissimus lumborum in Holstein bulls and steers with different beef qualities. PLoS One 15: e0235218, 2020.
36. Kanehisa M, Sato Y, Furumichi M, Morishima K and Tanabe M: New approach for understanding genome variations in KEGG. Nucleic Acids Res 47 (D1): D590-D595, 2019.
37. Mao X, Cai T, Olyarchuk JG and Wei L: Automated genome annotation and pathway identification using the KEGG orthology (KO) as a controlled vocabulary. Bioinformatics 21: 3787-3793, 2005.
38. Chettimada S, Lorenz DR, Misra V, Wolinsky SM and Gabuzda D: Small RNA sequencing of extracellular vesicles identifies circulating miRNAs related to inflammation and oxidative stress in HIV patients. BMC Immunol 21: 57, 2020.
39. Li X, Yuan L, Wang J, Zhang Z, Fu S, Wang S and Li X: MiR-1b up-regulation inhibits rat neuron proliferation and regeneration yet promotes apoptosis via targeting KLF7. Folia Neuropathol 59: 67-80, 2021.
40. Liu YP, Xu P, Guo CX, Luo ZR, Zhu J, Mou FF, Cai H, Wang C, Ye XC, Shao SJ and Guo HD: miR-1b overexpression suppressed proliferation and migration of RSC96 and increased cell apoptosis. Neurosci Lett 687: 137-145, 2018.
41. Macías M, Rebmann V, Mateos B, Varo N, Perez-Gracia JL, Alegre E and González Á: Comparison of six commercial serum exosome isolation methods suitable for clinical laboratories. Effect in cytokine analysis. Clin Chem Lab Med 57: 1539-1545, 2019.
42. Xi Y, Jiang T, Wang W, Yu J, Wang Y, Wu X and He Y: Long non-coding HCG18 promotes intervertebral disc degeneration by sponging miR-146a-5p and regulating TRAF6 expression. Sci Rep 7: 13234, 2017.
43. Zhang H, Zheng W, Li D and Zheng J: miR-146a-5p promotes chondrocyte apoptosis and inhibits autophagy of osteoarthritis by targeting NUMB. Cartilage 13 (2 Suppl): 1467S-1477S, 2021.
44. Liu J, Yu J, Jiang W, He M and Zhao J: Targeting of CDKN1B by miR-222-3p may contribute to the development of intervertebral disc degeneration. FEBS Open Bio 9: 728-735, 2019.
45. Fan H, Niu W, He M, Kong L, Zhong A, Zhang Q, Yan Y and Zhang L: Bioinformatics analysis of differently expressed microRNAs in anxiety disorder. Zhonghua Yi Xue Yi Chuan Xue Za Zhi 32: 641-646, 2015 (In Chinese).
46. Kao YC, Chen JY, Chen HH, Liao KW and Huang SS: The association between depression and chronic lower back pain from disc degeneration and herniation of the lumbar spine. Int J Psychiatry Med 57: 165-177, 2022.
47. Wei Q, Zhang X, Zhou C, Ren Q and Zhang Y: Roles of large aggregating proteoglycans in human intervertebral disc degeneration. Connect Tissue Res 60: 209-218, 2019.
48. Silagi ES, Shapiro IM and Risbud MV: Glycosaminoglycan synthesis in the nucleus pulposus: Dysregulation and the pathogenesis of disc degeneration. Matrix Biol 71-72: 368-379, 2018.